

Experimental Study of Wave Forces on an Offshore Wind Turbine Tower Model

Krishnil Ram, M. R. Ahmed
Division of Mechanical Engineering
The University of the South Pacific
Laucala Campus, Suva, Fiji

Young-Ho Lee
Division of Mechanical and Energy System
Engineering, Korea Maritime and Ocean University
727 Taejong-ro Youngdo-ku, Busan 49112, South
Korea

Abstract— A study of a tapered wind turbine tower is performed using particle image velocimetry and numerical methods. A 1.5 MW wind turbine base was studied and re-designed. A scaled model of a simple tapered tower base was studied in a wave channel using Particle Image Velocimetry (PIV) to understand the flow phenomena at the tower base. Theoretical and experimental results were found using Morrison equations. The diffraction parameter shows that the linear wave theory is not valid for inertial coefficient calculations. A direct value of 2.0 resulted for the inertial coefficient values while a lower drag influence was noted at coefficient of drag = 0.315. The turbine's horizontal force profile is improved in this study to yield a 69% reduction in overturning moment by redesigning the turbines submerged tower.

Keywords— Offshore wind turbine; Wave forces; Experimental study; Particle image velocimetry.

I. INTRODUCTION

Due to reduced wind velocities available onshore, wind turbine farms are not able to operate to their optimum level and hence the returns on investments are low. Onshore wind turbines have been found to create noise and interfere with communication devices. The Butoni Wind Farm in Sigatoka is an example of both these issues [1]. Major population areas that use most electricity cannot readily spare land for large scale installations as well. Offshore wind power has the capacity to allow large scale production of electricity for island nations. The velocity of wind offshore is much higher than on land [2]. An offshore wind turbine is defined as “a wind turbine with a support structure which is subject to hydrodynamic loading” [3]. Offshore wind turbines also have a greater area available for siting large projects near large population areas where land area is not easily available. Turbulence intensity at offshore locations is lower than locations on land [4]. This reduces fatigue loading on the wind turbine components. Lower wind shear allows shorter towers to be used thus reducing the material cost. For obvious reasons, wind turbines are often sited in sparsely populated areas on high ground, to take best advantage of the prevailing wind.

Unfortunately, these are just the locations that utility companies have chosen as microwave sites and scanning telemetry radio sites, and so turbines and radio sites are often in close proximity to one another [5]. With offshore wind turbines, communications signal interference is a lesser problem since they are located far from communications networks. Offshore wind technology is increasingly becoming popular in Europe and other nations that require utility scale power production. Pacific island nations including Fiji have an abundance of open sea area which provides a much higher velocity of wind, providing greater capacity for power generation. Having the towers at sea solves key issues such as visual impact and interference with communication.

However, the sea is one of the harshest environments to build a structure in. Offshore structures require a very large capital investment. The structural integrity of offshore towers is a vital part of designing these wind farms. This project aims to understand and investigate the relationship between the wave conditions and the resulting forces on the towers. It is very essential that we have an estimate of the type of loading. This study looks at approximating a suitable tower design for a location on the Western Coast of Viti Levu which can support a 1.5MW wind turbine. In order to understand the type of loading an offshore structure will withstand, one must have sufficient knowledge of the fluid flow around the structure and how the structure causes the fluid reactions. While the foundation costs make up for 5-10% of the onshore wind turbine costs, for offshore wind turbines this increases to 15 – 25% of the overall cost [6]. Hence the design of these towers needs to be economical as well as structurally sound to guarantee the viability of the wind turbine. There are three major components to an offshore wind turbine (OWT). These are the tower top Segment, tower marine segment and the foundation [4]. Figure 1 shows the major types of towers in use for shallow to medium depth applications. The choice of a particular OWT tower depends largely on the depth of installation. The major types of foundations used to hold the top and marine segments are gravity base and piles. Recently a lot of interest has been gained by a third type of foundation known as the suction bucket [5]. Suction buckets are tubular steel foundations that are installed by sealing the top and applying suction inside the bucket. The

hydrostatic pressure difference and the deadweight cause the bucket to penetrate the soil. This benign installation procedure allows the buckets to be connected to the rest of the structure before installation, enabling a reduction in steps of the installation procedure [7]. Above these foundations a variety of towers encompassing the marine and top segment, can be utilized. The common types of towers in use are monopile towers, which as the name suggests is made up of a slender cylindrical tower driven into the sea-bed using a pile foundation. Monopiles are economical in depths of up to 20m. But recently the application of monopiles has been stretched to deeper waters and larger turbines than anticipated possible, exemplified by the monopiles for the 3.6 MW turbines in 26 meters water depth at Arklow Bank [8]. Jacket-type substructures, which are lighter and stiffer in comparison to well-designed monopiles, are attractive solutions in water depths of about 20 to 50 meters [9]. Tripods can either have a pile or suction bucket foundation and comprise of three tubular members rising from the foundation to support a slender tubular tower. Mainly used in shallow water depths, gravity foundations resist the overturning loads solely by means of their own gravity. They are typically used at sites where installation of piles in the underlying seabed is difficult, such as on a hard rock ledge or on competent soil sites in relatively shallow waters. Gravity caissons are typically concrete shell structures [10]. The towers are constantly under load from the environment. Since the wind and waves come from the same direction, the greater danger in offshore wind turbines is not a vertical load but the overturning moment. The aerodynamic wind thrust force generated due to the rotors is given as:

$$F_t = \frac{1}{2} \rho_a \pi R^2 v_1^2 C_t(\lambda) \quad (1.0)$$

where C_t is defined as the co-efficient of thrust.

For OWT towers, as a proportion of the vertical loading, the horizontal loading and overturning moment are much larger [6]. Other loadings such as fatigue loading due to breaking waves and slamming loads have to be accounted for in the towers marine segment design as well as resonant effects on the top segment of the tower. In this study, specific attention is given to the horizontal loading on the marine segment and foundation due to the action of waves. In order to accurately predict the forces that a tower will endure in its service condition it is essential to have a reliable description of ocean waves for a particular location.

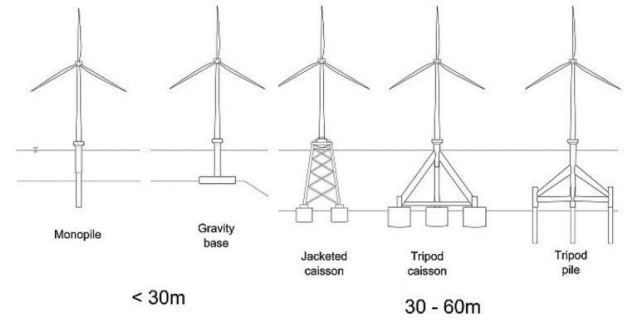


Fig 1. Major types of offshore wind turbine tower foundations [11].

The offshore wind turbine tower design standard DNV-OS-J101 recommends the use of the JONSWAP spectrum to describe the wave activity at a certain location [12]. The spectrum moments may be used to calculate key parameters such as H_s and T_p which are sufficient to characterise the complex wave activity at a location over a period of time. Depending on the situation the seabed slopes and geometry may need to be accounted for in separate equations (provided in DNV-OS-J101 [13]) before the final parameters are found to represent the wave activity.

1.1 Wave Kinematics for loading

Water waves are created by the shearing action of wind on the surface of the sea-water. The main characteristic of a wave are its period (T), height (H), and wave length (λ). In order to describe the motion of waves, several theories have been proposed. While the theories have their limitations, the trade off is usually between accuracy and complexity of the theory. The small amplitude wave theory, linear wave theory or Airy's Theory is a common tool used by engineers to obtain useful data about waves quickly by linearizing the description of wave propagation. There are many other higher order wave theories in use. There are mainly three parameters that can be used to determine which theory is applicable to a particular wave problem. Three wave parameters determine which wave theory to apply in a specific problem. These are the wave height H , the wave period T and the water depth d . These parameters are used to define three non-dimensional parameters that determine ranges of validity of different wave theories [6]. The Wave Steepness parameter (S), shallow water parameter (μ) and Ursell Number (U_r) are defined as follows:

$$S = 2\pi \frac{H}{gT^2} \quad (1.1)$$

$$\mu = 2\pi \frac{d}{gT^2} \quad (1.2)$$

$$U_r = \frac{1}{4\pi^2} \frac{S}{\mu^3} \quad (1.3)$$

For this study, only shallow water waves will be looked at. Shallow water is assumed when the $d < \lambda /20$, where d is the water depth. While water particles in deep water waves orbit in a circular path, shallow water orbits are seen to be elliptical. A water wave is assumed to be sinusoidal in the Linear wave theory and the horizontal component of velocity (U) is given as:

$$U(x, z, t) = a\omega \frac{\cosh(k(h+z))}{\sinh(kh)} \sin(at - kx) \quad (1.4)$$

The vertical component of the velocity (W) is given as:

$$W(x, z, t) = a\omega \frac{\sinh(k(h+z))}{\sinh(kh)} \cos(at - kx) \quad (1.5)$$

The derivative of the horizontal components velocity with respect to time gives the local acceleration of the particle at that point.

$$\frac{\partial U}{\partial t} = \dot{U} = a\omega^2 \frac{\cosh(k(h+z))}{\sinh(kh)} \cos(at - kx) \quad (1.6)$$

A similar result is obtained for the W component; however it contributes little to the wave loading calculations. The Morison equation which was developed in 1950 can be used to determine the inline force parallel to the direction of fluid flow. The equation is given in [13] as:

$$F_w = \frac{1}{2} \rho C_d D U |U| + \rho (C_m + 1) A \dot{U} \quad (1.7)$$

The coefficient of inertia and drag C_m and C_d need to be determined experimentally and used to predict the inline force caused by wave the wave action. Several methods have been proposed to numerically determine the value of the coefficients [16]. There is a vertical force that arises due to the weight of the turbine structure itself. Equation 1.7 can only be used safely when the *diffraction parameter* for the slender cylinder is less than 0.2. Since all three forces are now defined for the tower, Figure 2 gives a visual representation of the forces on the tower.

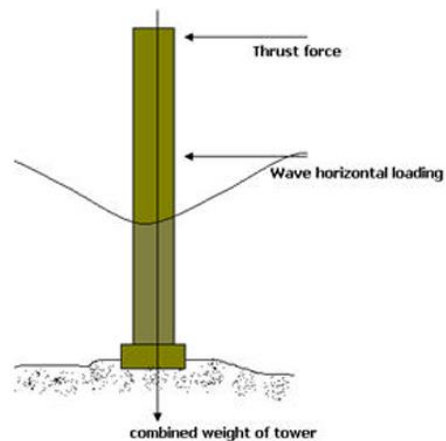


Fig 2. Forces on a GBS tower

Other forces such as those due to buoyancy can be assumed negligible. This study looks at ways in which experimental values for C_d and C_m are found for tapered tower geometry.

II. METHODOLOGY

For the experiment a base model for a 1.5MW OWT was selected from the NREL series of WindPACT towers [15]. The base diameter of the turbines are 4.9 m with a taper to 4.3 m in the first section of the tower. For this study the later sections exposed to wind loads are not considered. A 1:100 scale model of the tower's marine segment was built. The base diameter of the tapered model was 49mm while the top diameter at a length of 215mm was 43mm. The tower was allowed to extend above this diameter for another 100mm to avoid overtopping since only a section of the entire tower was being tested. The experiment was designed to understand the flow of fluid around the marine segment of the tower. The wave channel used in this experiment is 300mm wide, 3500mm long and 400mm deep. The tower model was tested at a depth of 260mm which gave a depth of 160mm on the platform. Wave frequencies of 0.8, 1.0 and 1.2 Hz were tested. The schematic in Figure 3 shows the experimental setup.

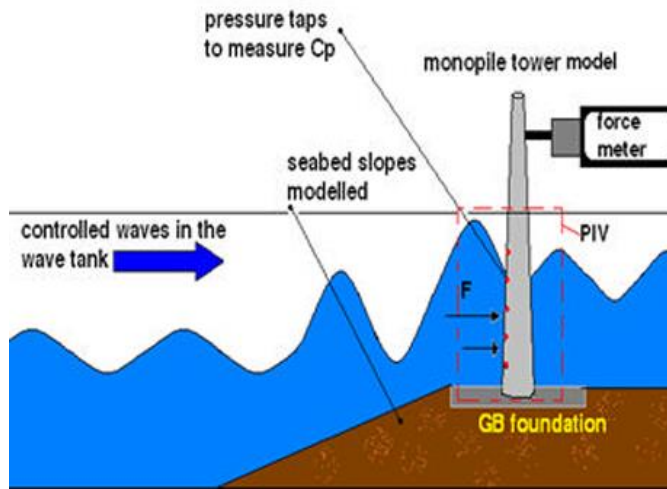


Fig 3 Wave Flume Experimental Setup

Part of the Morrison equation requires the determination of horizontal velocity component. There are several ways to measure the velocity of a fluid. Particle Image Velocimetry (PIV) requires seeding of similar density solid particles into the fluid. A target area in the fluid is illuminated twice with a known time step. At each light pulse an image of the particles in the target area is made. By comparing two successive images the displacements of each particle can be determined. Since the time step is known, the velocity could be calculated. For this experiment, a 4 watt 532 nm green light solid-state continuous laser was used along with a camera operating at 200 fps. Poly-Vinyl Chloride (PVC) particles, with an average diameter of 100 μm and specific gravity of 1.02 were used for seeding the flow. Figure 3 shows the 2D display of the target area for the camera while figure 4 describes the setup for PIV measurements.

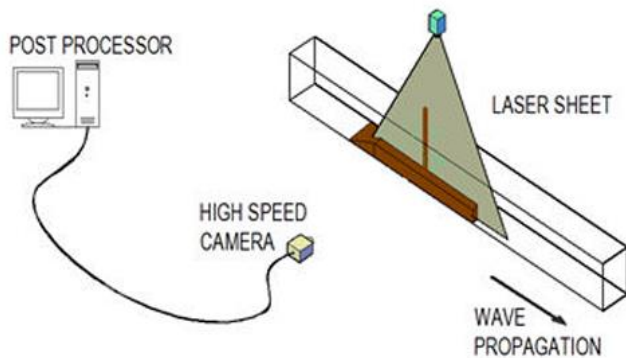


Fig 4. PIV measurement setup.

PIV results were used to determine the horizontal velocity components and to visualize the flow around the turbine tower. The factors which were considered for determining the accuracy of velocity measurements with PIV are: the uncertainties due to finite time sampling, finite displacement of the particles, and uncertainties in measuring the displacements

of the particle images [16]. The accuracy of displacement measurements with Cactus is of the order of 0.1 pixel. For the high-speed camera, the time resolution for the current measurements was 0.008 s. To get an accurate estimate of the error in our measurements, PIV measurements were performed on a calibrated, constant speed rotating motion and the maximum error was found to be 0.32%.

III. RESULTS AND DISCUSSION

PIV results show the behavior of the particles and their elliptical orbits without the tower in place at a frequency of 1.2 Hz (extreme wave condition) in Figure 5.

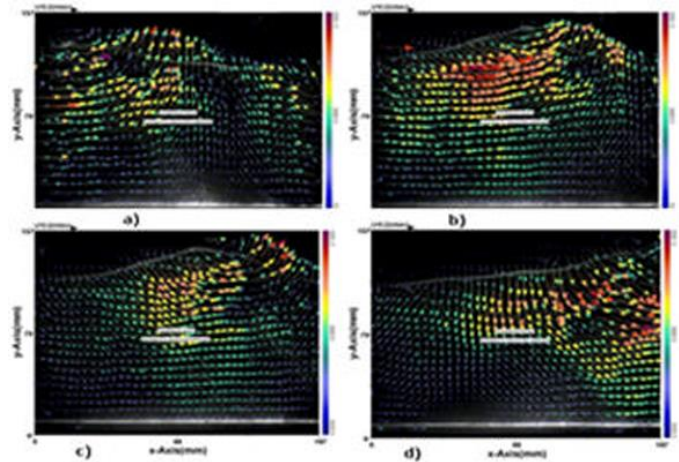


Fig 5. PIV results at 1.2Hz . The results show the particle behavior in waves for phase angles of 0, $\pi/3$, $2\pi/3$ and π .

The particle velocities were also observed when the tower model was placed on the platform. At a frequency of 1.2 Hz, a wave height of more than 65mm was generated and made to impact the tower. Figure 6 shows the same phase angles with the tower as the obstacle. In order to capture a detailed image of the velocities, the frame size was reduced and focused on the front of the tower.

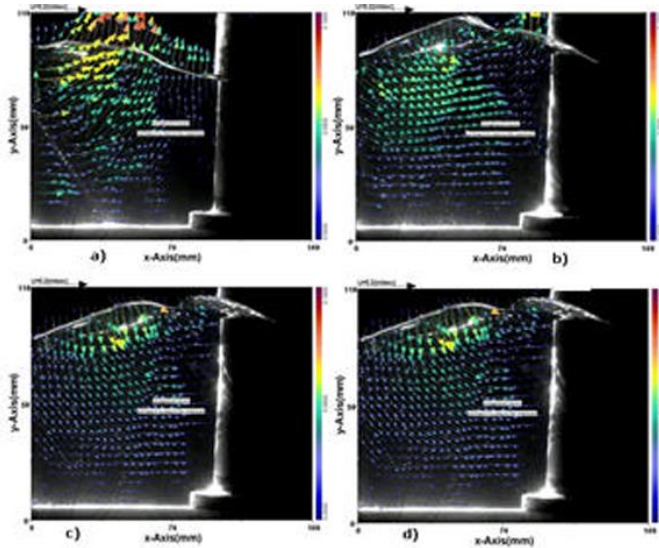


Fig 6. PIV results of wave impact on the tower at 1.2 Hz . The results shows the particle behavior in waves for phase angles of 0, $\pi/3$, $2\pi/3$ and π .

The Linear wave theory also allows a theoretical calculation of the horizontal velocity component U using equation 1.4. The maximum horizontal velocity was calculated and compared with the velocities obtained from PIV results. Table 1 summarizes the velocity values obtained for the 1.2 Hz case. The values of velocity taken while the tower is in place are lower due to the wave interaction with the tower. As the wave impacts the tower, a stagnation point is generated on the impact side of the tower and since the approaching fluid is also slowed down, the reduction in velocity occurs.

TABLE I
HORIZONTAL VELOCITIES FROM PIV AND LINEAR WAVE THEORY

max u velocity under crest m/s								
calculated		PIV		PIV w/o		K	C	
		with		tower				
		tower						
0	π	0	π	0	π			
0.089	-	0.09	-0.05	0.0	0.075	9	1	$\frac{47}{2}$
0.124	-	0.12	-0.09	0.1	0.08	3	12	$\frac{77}{2}$
0.1719	-	0.17	-0.14	0.1	0.12	65	17	$\frac{3}{18}$

The Keulegan – Carpenter (KC) number is an important parameter for determining the influence of the drag and inertial forces. KC values are essential in determining the C_d and C_m for the tower.

$$KC = \frac{U_{\max} T}{D} \quad (1.8)$$

TABLE 2
DIFFRACTION AND STEEPNESS PARAMETERS

H cm	f	D	L	h/D	L/D	D/L
4.6	0.8	4	1.9	1	44.	0.0226
		.5	9		2	
5.54	1	4	1.5	1.	35.	0.0283
		.5	9	2	3	
7.4	1.2	4	1.3	1.	29.	0.0341
		.5	2	6	3	

In order to determine the effect of diffraction in this case, a diffraction parameter (D/L) needs to be calculated for the tower. Chu [17] determined that for $D/L < 0.2$, the linear wave theory is no longer valid and the C_m value can be taken as 2.0. Similarly the equation for C_m is defined as a composite function by Chu and after determining the steady flow drag coefficient C_d an approximation of the C_d value can be made using C_d and KC . The C_d value approximated in this case came to 0.315. These values of C_m , C_d , U , and dU/dt were substituted into the Morison equation to yield the horizontal force profile for the tower. Figure 7 shows the force profile on the marine segment of the OWT.

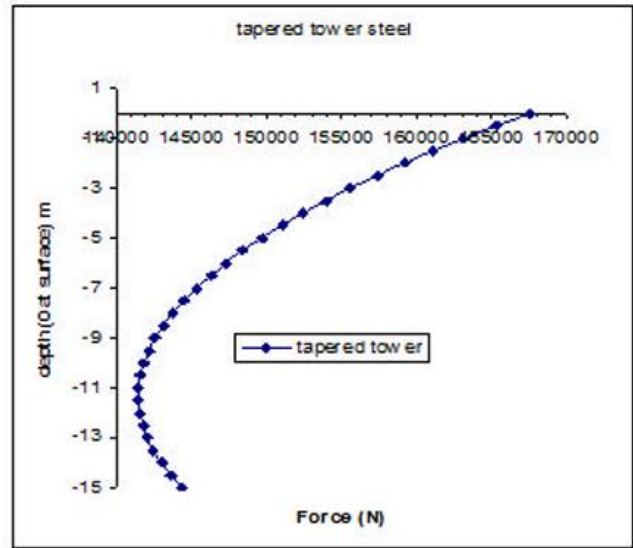


Fig 7. Horizontal force distribution till a depth of 15m. Extreme cyclone wave conditions of the coast of Viti – Levu were used with a H_s of 7.4m and T_p of 10s.

The overturning moment caused by the force distribution comes to 51.75MN-m given that the resultant of the load profile acts at a depth of around 3.5m. After redesign using various geometric changes, a new design of the marine segment was generated. The force profile for the new design is given in Figure 8.

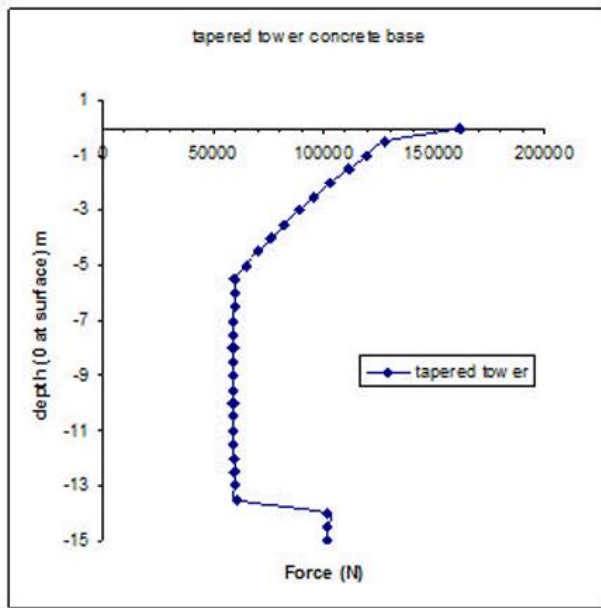


Fig 8. Horizontal force profile for the newly designed tower.

The changes in geometry cause a 69% reduction in overturning moment. The overturning moment for this design is calculated to be 19.28MNm. This is achieved by shifting the resultant force closer to the base of the tower. In this case the resultant now acts at a depth of 7m. The tower diameter under the wave is reduced to minimize the drag forces. An inverse taper was used to ensure that the top section dimensions do not get affected by the changes in the marine segments. Reducing the overturning moments at the marine segments allows the top segment to take up an extra 69% thrust force. This also means that higher lift blade sections can be used since the tower now has a greater capacity to counter the thrust component. The dimensions of the new geometry are provided in Fig. 9.

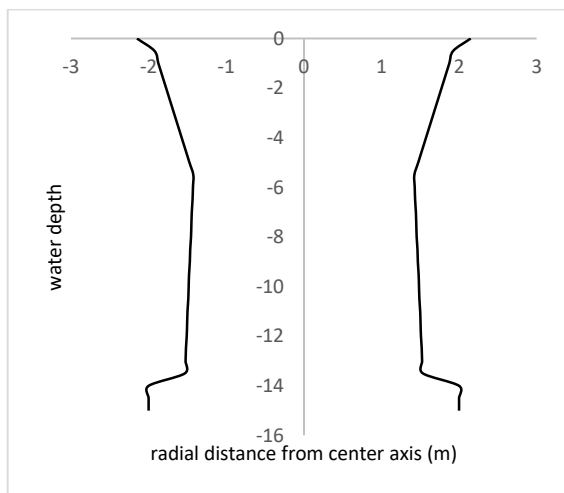


Fig 9. Proposed geometry of marine segment

IV. CONCLUSION

A scaled down turbine tower model was experimented on to determine C_d and C_m values. The C_m and C_d values were used to generate and optimize the horizontal force profile to design a new marine segment for a 1.5 MW tower. The new segment boasts a 69% reduction in overturning moment which adds to its economic and structural viability. The submerged section diameters were determined from Morison equations and using local sea states. Further structural analysis of the tower is in progress.

REFERENCES

- [1] A Kumar, T Weir, Wind power in Fiji – A preliminary analysis of Butoni wind farm. International Solar Energy Society Conference, October, Sydney-Australia, 2008.
- [2] " Technical Assessment of Onshore and Offshore Wind Generation Potential in New England" Levitan and Associates, Inc. pp. 7, 2007
- [3] C.N Elkinton and J.G McGowan, An Overview of Offshore Wind Energy. Renewable Energy Research Laboratory, University of Massachusetts.
- [4] .Nino and P Eecen . "ECN-DOWEC Turbelence and Wind Shear, A Literature Study and measurements ," DOWEC-F1W1-PE-01-044/00 P.
- [5] G.T Houlby and B.W Byrne, Suction Caisson Foundations for Offshore Wind Turbines and Anemometer Masts, Wind Engineering, 24 (4) (2000) 249-255.
- [6] M Junginger , A Faaji and W C Turkenburg, Cost Reduction Prospects for Offshore Wind Farms, Wind Engineering, 28 (1) (2004) 97-118.
- [7] M.B Zaaier ,Suction Bucket Foundation –Feasibility and pre-design for 6MW DOWEC, Ducth Offshore Wind energy Converter Project, (2002), 4-8
- [8] M.B Zaaier, Review of Current Activities In Offshore Wind Energy, Centrum for Vlnbruk, 2004.
- [9] M Zhang., H Li., P Li . and S L J Hu , Fundamental Structural Frequency Analysis for Jacket-Type Offshore Wind Turbine. Proceedings of the twentieth (2010) International Offshore and Polar Engineering Conference.
- [10] S Malhotra, Design and Construction Considerations for Offshore Wind Turbine Foundations in North America. Geo Florida (2010), 1533-1542. doi: 10.1061/41095(365)155.
- [11] S Bhattacharya, Challenges in design of foundations for Offshore Wind Turbines. Engineering & Technology Reference, (2014). 1(1).
- [12] K Horikawa , Coastal Engineering – An introduction to Ocean Engineering, John Wiley & Sons, (1978) 42-180.
- [13] Veritas, DNV-Det Norske. "DNV-OS-J101 offshore standard." Design of Offshore Wind Turbine Structures (2010).
- [14] B M Sumer and J Fredsoe "Hydrodynamics around cylindrical structures," Advanced Series on Ocean Engineering, vol. 26, World Scientific Publishing, 2006.
- [15] J M J Journee and W W Massie, "Offshore Hydromechanics. Technical Report," Delft University of Technology , www.ocp.tudelft.nl, January 2001.
- [16] JM Raffel, , C Willert,, J Kompenhans, 1998. Particle Image Velocimetry-A Practical Guide, 1st ed. Springer, Berlin Heidelberg.
- [17] V Chu and C Mei, On slowly-varying Stokes waves. *Journal of Fluid Mechanics*, 41(4), 873-887. doi:10.1017/S0022112070000988, (1970).